

SEISMIC CONTROL OF POST-TENSIONED ROCKING WALLS WITH INERTERS

Rodrigo THIERS-MOGGIA¹, Christian MÁLAGA-CHUQUITAYPE²

Abstract: *The allowance of controlled uplifting and rocking in structures can reduce the seismic shears and moments that develop at their base in the case of strong ground shaking. During the last decades, this concept has been widely applied to the development of hybrid post-tensioned buildings that can control the structural damage during severe earthquakes. One of such applications are post-tensioned rocking walls where the structural members are free to uplift and rock while post-tensioned tendons are incorporated to increase the lateral resistance and re-centring capabilities of the structure. Although the incorporation of the tendons help to control lateral deformations, preliminary results suggest that they also increase peak floor accelerations, which can result in excessive non-structural and contents damage. One alternative to reduce seismic-induced deformations and floor accelerations in rocking structures is the incorporation of supplemental rotational inertia devices. The proposed strategy employs inerters, a mechanical device that develops a resisting force proportional to the relative acceleration between its terminals. In this paper, we assess the potential advantages of using inerters to further reduce the seismic rotation demands and offset the increases in floor accelerations brought about by the vertical post-tensioning in rocking structures. Our study shows that the inclusion of the inerter has an effect equivalent to reducing the frequency parameter of the structure, resulting in an enhanced seismic stability due to the well-known size effect of rocking behaviour.*

Introduction

Controlled rocking of structures can significantly reduce the seismic shears and moments that develop at their base when subjected to strong ground shaking. During the last decades, this concept has been widely applied to the development of hybrid post-tensioned connections that can improve the seismic performance of civil structures. Although the system has shown to be effective in controlling structural damage, high rotations and accelerations associated with the rocking motion can cause significant non-structural and contents damage. One alternative to tackle this issue is the incorporation of a relatively new seismic control device named inerter. The inerter is a linear mechanical element that develops a resisting force proportional to the relative acceleration between its terminals (Smith, 2002). During the last decades, several inerter-based dampers have been proposed combining inerters with springs, tuned mass dampers and viscous energy dissipation (Giaralis and Taflanidis, 2015) or clutch systems (Málaga-Chuquitaype *et al.*, 2019). When amplifying mechanisms such as ball-screws (Ikago *et al.* 2012) or geared wheels (Makris and Kampas 2016) are used, high levels of vibration isolation can be achieved with low amounts of added mass.

In this paper, we investigate the potential advantages of using supplemental rotational inertia to mitigate the effects of earthquakes on post-tensioned rocking structures. Firstly, we present a simplified single-degree-of-freedom system representative of rigid post-tensioned rocking walls equipped with inerters and derive the equations that describe its rocking motion. This model is then used to examine the basic dynamic behaviour of such structures when subjected to acceleration pulses and real pulse-like earthquakes ground motions. Finally, the efficiency of the proposed system is assessed comparing the rotation and floor acceleration response of a 3-storey Cross-Laminated-Timber Rocking-Walled building with and without inerters.

Simplified SDOF Model of a Post-tensioned Rocking Wall

The general dynamic characteristics of post-tensioned rocking structures can be studied considering a rigid block (Housner, 1963) connected to a fixed base through a vertical tendon

¹ PhD Candidate, Imperial College, London, United Kingdom, r.thiers16@imperial.ac.uk

² Senior Lecturer, Imperial College, London, United Kingdom

(Vassiliou and Makris, 2014). The dynamic response of such system under the action of a base pulse can be expressed as a function of six dimensionless groups:

$$\theta(t) = f\left(\frac{\omega_g}{p}, \tan \alpha, \frac{a_g}{g}, \frac{EA}{mg}, \frac{P_0}{mg}, pt\right) \quad (1)$$

where ω_g and a_g are the frequency and acceleration amplitude of the ground excitation; p and α are the frequency parameter and slenderness of the wall, respectively; and EA and P_0 represent the elasticity and initial post-tensioning force of the vertical tendon.

An inerter can be easily introduced into this system by connecting the terminals of the device to the fixed base and the rocking body as proposed by Thiers-Moggia and Málaga-Chuquitaype (2019) for free-rocking bodies. One possible configuration is shown in Figure 1.

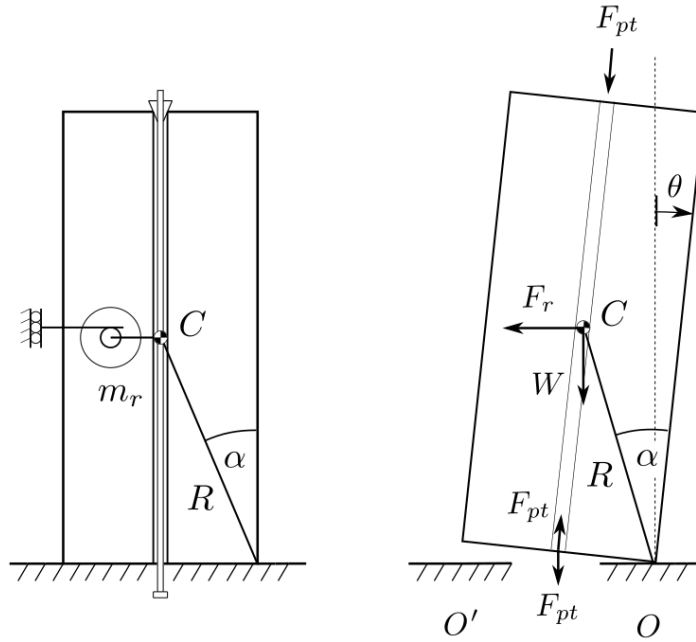


Figure 1. Single-degree-of-freedom model of a post-tensioned rocking wall connected to an inerter.

The force in the post-tensioned tendon, F_{pt} , is obtained as the sum of the initial post-tensioning and the deformation-induced forces:

$$F_{pt} = EA \tan \alpha \frac{\sqrt{2}}{2} \sqrt{1 - \cos \theta} + P_0 \quad (2)$$

On the other hand, the resisting force in the inerter, F_r , can be estimated as the product between the inertance, m_r , and the relative linear acceleration between the inerter terminals:

$$F_r = m_r R \ddot{\theta} \cos(\alpha \operatorname{sgn}(\theta) - \theta) \quad (3)$$

If slender structures are considered ($\alpha < 20^\circ$), the rotation response of such system is described by:

$$\ddot{\theta} = -p_\sigma^2 \left(\alpha \operatorname{sgn}(\theta) \left(1 + \frac{P_0}{mg} \right) + \theta \left(\frac{EA\alpha^2}{2mg} - 1 \right) + \frac{\ddot{u}_g}{g} \right) \quad (4)$$

with

$$p_\sigma = \sqrt{\frac{3g}{R(4 + 3\sigma)}}$$

where R is the size parameter of the block, and $\sigma = m_r/m$ is the apparent mass ratio of the inerter. In this case, an inerter connected to the centre of mass of the block has been considered for clarity.

Equation 4 shows that the inclusion of the inerter has an effect equivalent to reducing the frequency parameter, p , of the block (Thiers-Moggia and Málaga-Chuquitaype, 2019). In general, the reduction of the frequency parameter should result in lower seismic demands due to the size effect of rocking behaviour. This principle dictates that among two blocks of the same slenderness α , the one with the lower frequency parameter, p (larger in size), is more stable and therefore has lower levels of relative structural demands. It is important to note that for a given rectangular block, the frequency parameter, p , depends only on the size, R , and therefore cannot be modified without altering its geometry. Consequently, the use of supplemental rotational inertia devices configures a practical alternative to enhance the dynamic response and reduce seismic demands in rocking structures.

Response under Pulse Ground Accelerations

Rocking spectra were obtained for a wide range of Ricker pulse excitations (Ricker, 1943) in order to assess the dynamic response of post-tensioned rocking structures equipped with inerters. To this end, we considered different levels of pre-stress (P_0) and elastic force (EA), resulting in structural stiffnesses that vary from negative to positive values. Additionally, an inerter of apparent mass $\sigma = m_r/m = 1$ was examined to evaluate the effect of the proposed seismic control strategy. The response was studied in terms of maximum rotation and peak angular acceleration. Figure 2 shows the results obtained for walls of positive post-uplift stiffness ($EA/mg = 3 / \tan^2 \alpha$), for two different levels of initial post-tensioning force.

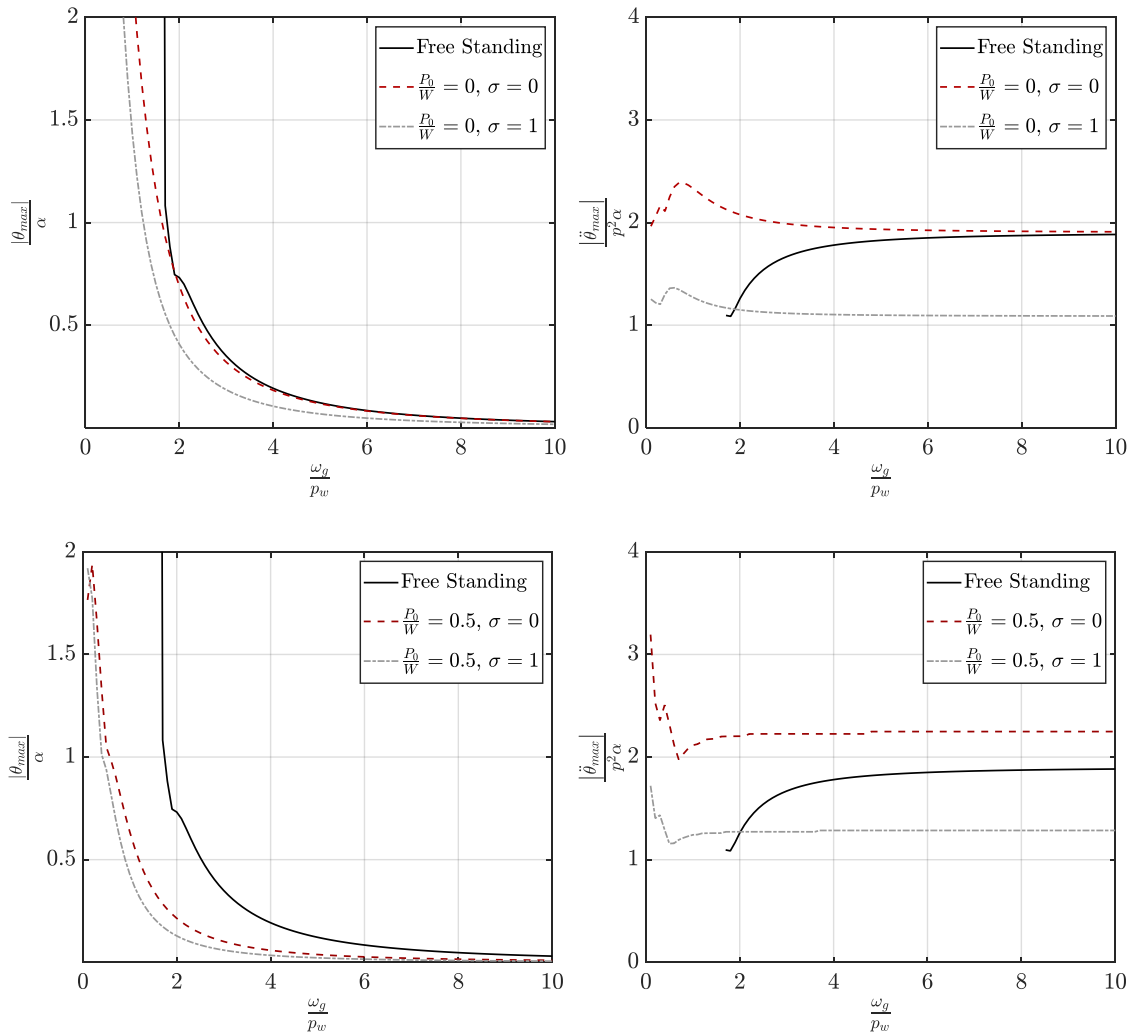


Figure 2. Rotation (left) and angular acceleration (right) response of post-tensioned rocking blocks of positive post-uplift stiffness ($EA/mg = 3 / \tan^2 \alpha$) subjected to Ricker pulse excitations.

The results presented in Figure 2 show that the elastic force (EA/mg) improves the stability of the block when $\omega_g/p < 2$ (small structures), but has little effect on the maximum rotation and

acceleration response for bigger blocks. This behaviour is related to the increase in the post-uplifting stiffness, which allows the block to withstand rotations greater than α and still return to its vertical position. Nevertheless, higher rotational accelerations were observed for some small to medium-sized blocks ($\omega_g/\rho < 4$).

On the other hand, the level of initial post-tensioning force (P_0/mg) has a more significant effect on the maximum rotation response of both, small and large structures. While an improved stability was observed for $P_0/mg = 0.5$, reductions in the maximum rotations for greater frequency ratios (larger blocks) were also obtained. Importantly, the response enhancement becomes more significant the higher the level of initial post-tensioning force. However, these improvements happen at the expense of inducing higher rotational accelerations for most of the frequency ratios analysed when $\sigma = 0$.

Additionally, the results presented in Figure 2 show that the inerter further reduces the rotation demands of the post-tensioned rocking structures, while at the same time it offsets the increment in peak angular accelerations brought about by the initial post-tensioning force. Moreover, the maximum angular accelerations obtained for the post-tensioned structure equipped with the inerter (i.e. $P_0/mg = 0.5$ and $\sigma = 1$ in Figure 2) are consistently lower than the demands of the benchmark free-standing rigid block. These results show that the use of inerters can be particularly attractive for controlling rotation and acceleration seismic demands in post-tensioned rocking structures.

Response under Real Pulse-like Earthquake Ground Motions

During actual seismic events, structures are subjected to acceleration histories that can be represented as series of individual pulses with different frequencies. The early work of Housner (1963) already identified that the action of these successive pulses can increase the structural demands and overturn free-standing blocks for smaller acceleration amplitudes than a single pulse excitation. In this section, we assess the effectiveness of the inerter for the protection of rocking structures for a set of 7 pulse-like ground motion records obtained from the Pacific Earthquake Engineering Research Center (PEER) database. Table 1 summarizes the catalogue of earthquakes used in the analyses.

Earthquake name	Year	Magnitude M_w	Mechanism
San Fernando	1971	6.6	Reverse
Tabas, Iran	1978	7.4	Reverse
Imperial Valley	1979	6.5	Strike Slip
Morgan Hill	1984	6.2	Strike Slip
San Salvador	1986	5.8	Strike Slip
Superstition Hills	1987	6.5	Strike Slip
Loma Prieta	1989	6.9	Reverse Oblique

Table 1. Earthquake ground motion database

A 3-storey rigid-wall system ($R = 9[m]$, $\alpha=10^\circ$) with positive post-uplift stiffness ($EA/mg = 3 / \tan^2 \alpha$) and $P_0/mg = 0.25$ was selected as a realistic case of study, while an inerter of apparent mass ratio $\sigma = 1$ was considered for the protected cases. Figure 3 compares the dimensionless rotation and acceleration response histories of the structures subjected to the 1984 Morgan Hill earthquake record.

The results plotted in Figure 3 and Figure 4 are consistent with the observations made in the previous sections for Ricker pulse excitations. While the addition of the post-tensioned tendons reduced the maximum rotation of the wall it also increased the peak acceleration. Nevertheless, the introduction of the inerter efficiently offsets this effect, further lowering the rotation response and significantly reducing accelerations to levels even lower than the benchmark free-standing structure.

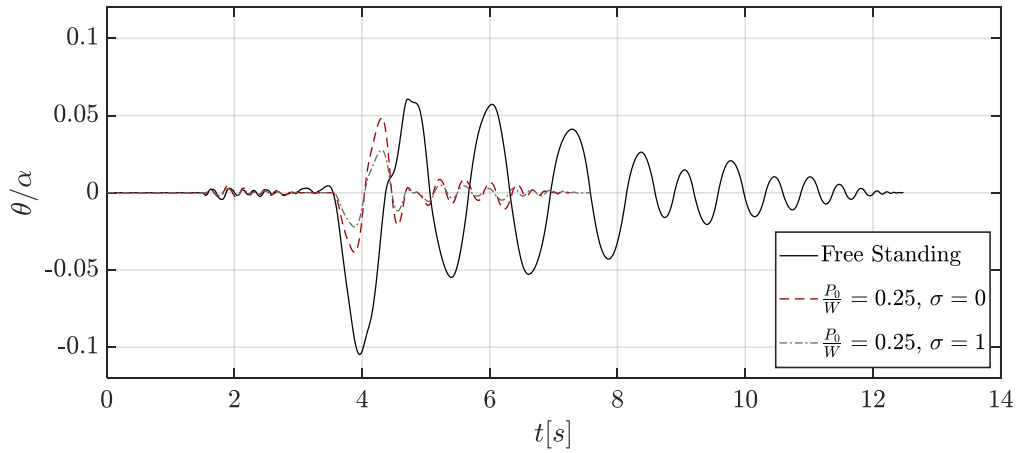


Figure 3. Rotation response of the practice-representative rocking walled structure.

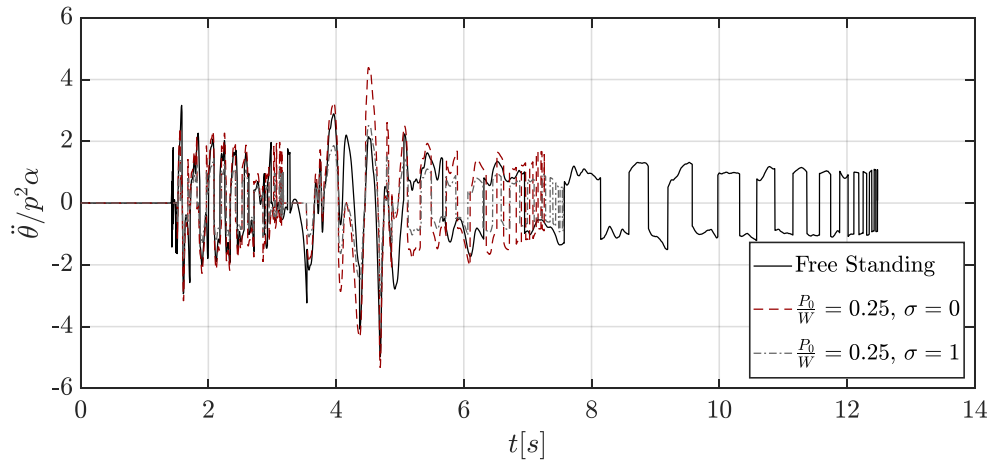


Figure 4. Acceleration response of the practice-representative rocking walled structure.

Similar analyses were conducted for all earthquake ground motions listed in Table 1, which results are summarized in Figure 5. The rocking response of the structures is characterized in terms of dimensionless values of maximum rotation and peak angular acceleration. These are presented as a function of p times the uniform duration, t_{uni} . This ground-motion intensity measure corresponds to the sum of the time intervals during which the ground acceleration exceeds the limit to cause uplifting, and has been shown to strongly correlate with structural demands in rocking structures (Dimitrakopoulos et al. 2018).

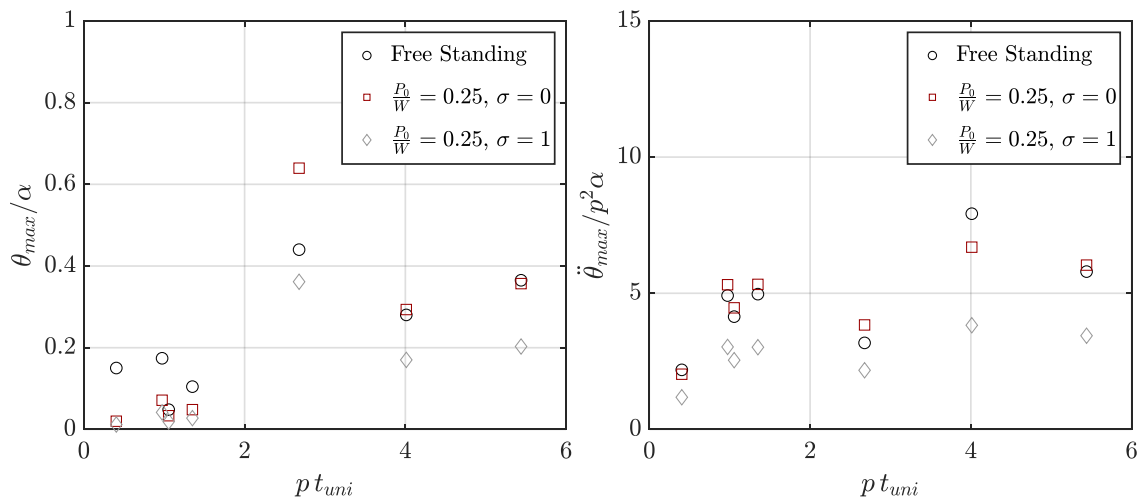


Figure 5. Summary of rotation and angular acceleration demands for the earthquake database.

Figure 5 shows that the introduction of the vertical tendon reduces rotation demands for lower intensities, but has a less significant impact for higher values of pt_{uni} . On the other hand, most of the post-tensioned cases registered increased angular accelerations when compared to the free-standing case. Importantly, all the structures equipped with inerters experienced consistently low peak rotation and angular acceleration demands.

Case of Study: 3-Storey Rocking CLT Walled building

Definition of the structural system

A 3-Storey Rocking CLT Walled building is considered in order to numerically assess the proposed seismic control strategy in a realistic rocking structure. The building is formed of rectangular 10x12-meter modules with an inter-storey height of 3 meters, as shown in Figure 6. The structural plan consists of two frames in the Y direction supporting gravity loads, and two UFP-coupled post-tensioned CLT walls providing lateral load resistance in the X and Y directions. The length, L_w , and width, e , of each wall panel are design parameters. Additional details about the building can be found in Thiers-Moggia and Málaga-Chuquitaype (2018)

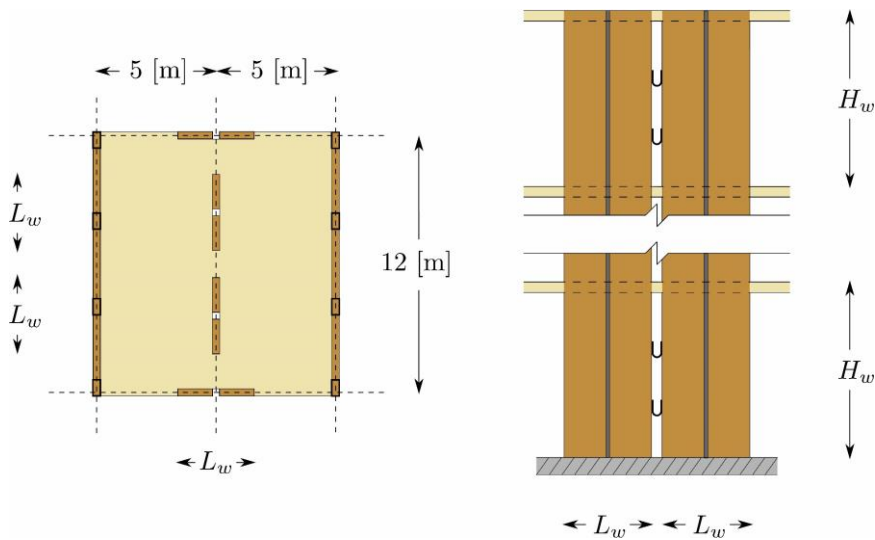


Figure 6. Plan and elevation view of the structural system considered (Thiers-Moggia and Málaga-Chuquitaype, 2018).

The coupled post-tensioned timber walls were designed following Direct Displacement Based Design (DDBD) guidelines (Newcombe, 2011). The results of the design procedure are summarized in table 2.

L_w [m]	e [m]	A_{pt} [cm ²]	P_0 [kN]
1.5	0.18	2.8	230

Table 2. Design parameters of the case-of-study building.

Numerical Models

The analytical model for coupled post-tensioned walls proposed by Newcombe (2011) was adapted and implemented in OpenSees (Mazzoni et al., 2009). The structural system can be divided in three main components: timber walls, post-tensioned tendons, and UFP coupling devices. A schematic diagram of the model is shown in Figure 7.

On the other hand, the numerical formulation proposed by Thiers-Moggia and Málaga-Chuquitaype (Thiers-Moggia and Málaga-Chuquitaype, 2018, Málaga-Chuquitaype et al., 2019) was used to simulate the inerter devices. This model consists of two nodes connected through a rigid link, and an angular mass assigned to the rotational degree of freedom of the system. A schematic diagram of the model is shown in Figure 8.

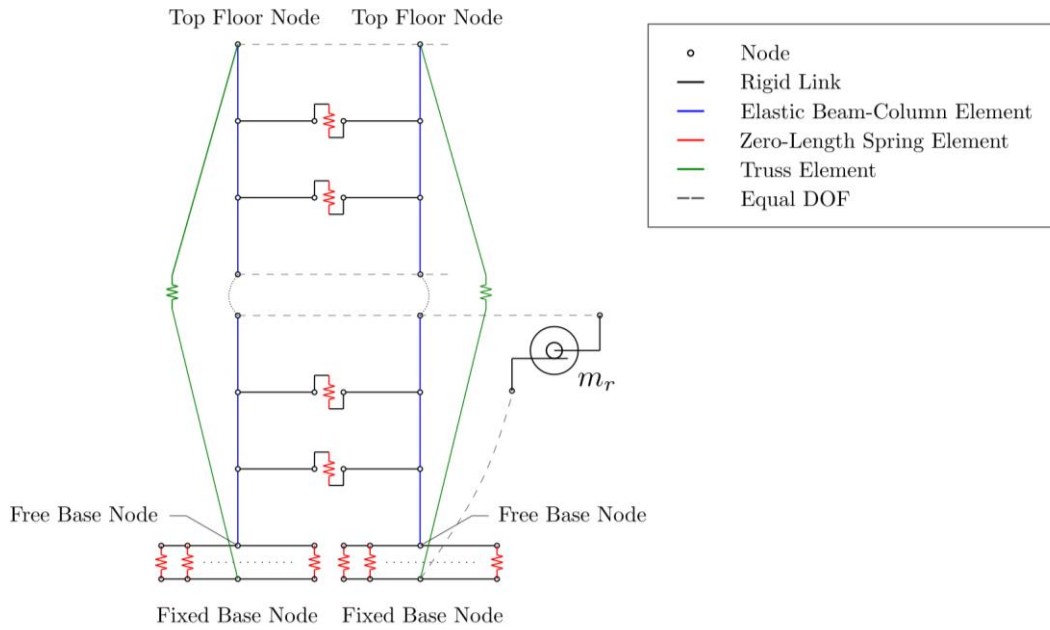


Figure 7. Numerical model of the coupled post-tensioned timber wall system.

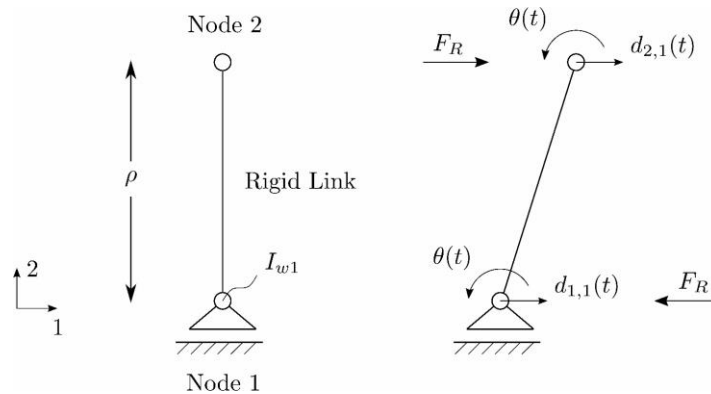


Figure 8. Schematic diagram of the numerical model for the inerter (Thiers-Moggia and Málaga-Chuquitaype, 2018, Málaga-Chuquitaype et al., 2019).

Response under Real Pulse-like Earthquake Ground Motions

The post-tensioned walled building described in the previous section was subjected to the earthquake ground motion database defined in Table 1. A single grounded inerter of apparent mass ratio $\sigma=0.33$ connected to the first floor as shown in Figure 7 was used for the protected structure. Although the apparent mass of the device may seem high, the actual gravitational mass can be reduced many orders of magnitude if amplifying mechanisms such as ball-screws or geared wheels are used (Makris and Kampas, 2016).

Figure 9 presents the results obtained for the protected and unprotected structures subjected to the 1984 Morgan Hill earthquake record. The left plot in Figure 9 demonstrates significant reductions in peak inter-storey drifts along the height of the building brought about by the inerter. Importantly, the displacement profile remains approximately linear, in agreement with the design assumption. On the other hand, peak floor accelerations are described in terms of the floor acceleration magnification factor (FAM), which correspond to the ratio between the peak floor acceleration (PFA) and the peak ground acceleration (PGA). Again, important reductions are observed along the three floor levels.

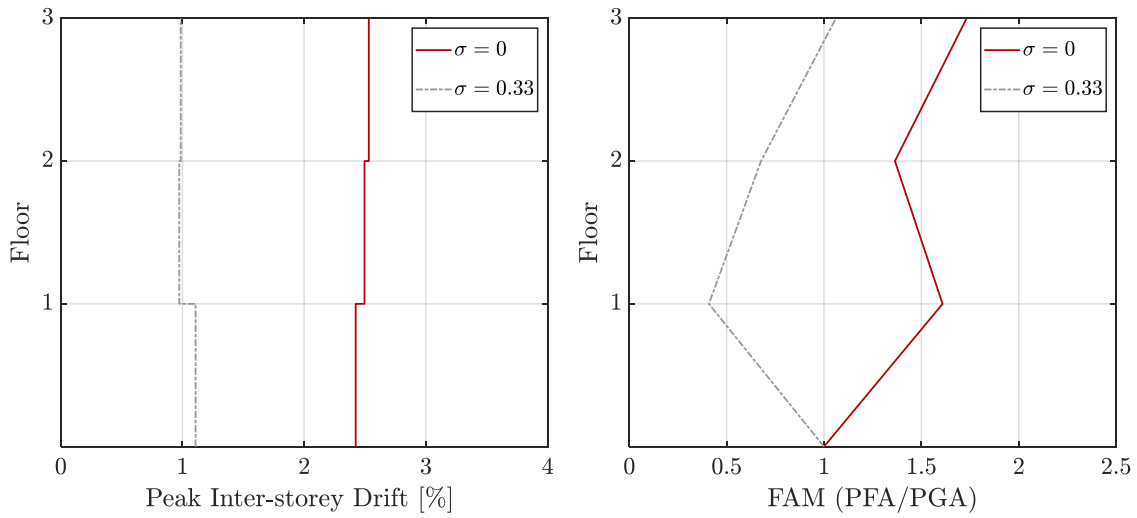


Figure 9. Maximum response parameters for the 1984 Morgan Hill earthquake record.

Figure 10 summarizes the results of the response history analyses. The performance of the structures is compared in terms of maximum inter-storey drift and peak floor accelerations. The uniform duration, t_{uni} , is adopted as the intensity measure. To this end, the uplifting limit required for its calculation was obtained theoretically as:

$$\ddot{u}_g \geq \frac{P_0 + W}{m_{sis}} \tan \alpha \quad (5)$$

where m_{sis} is the seismic mass of the structure.

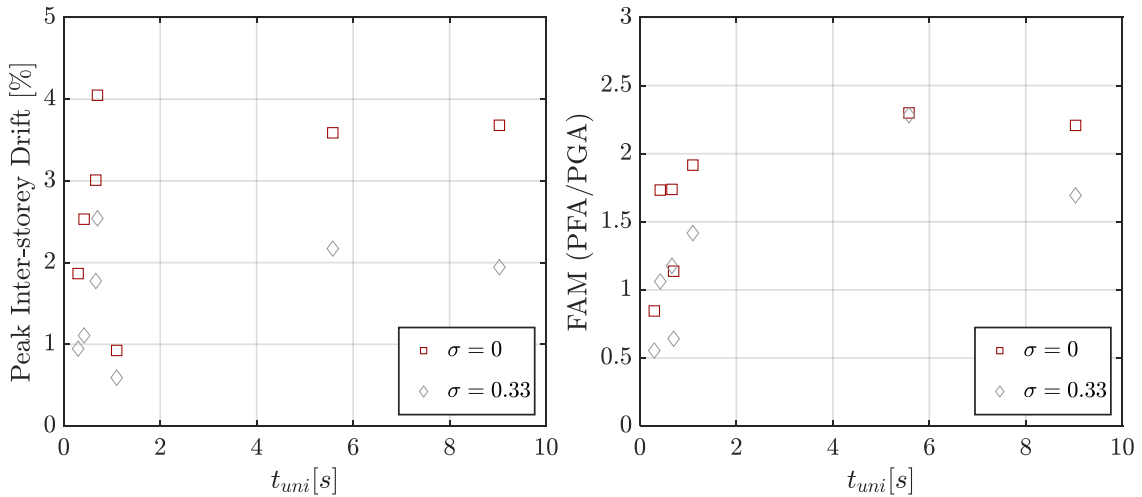


Figure 10. Summary of rotation and angular acceleration demands for the earthquake database.

The results obtained by means of the detailed numerical model of the 3-stories rocking building are consistent with the findings for the simplified single-degree-of-freedom systems. Significant reductions are observed for both, inter-storey drifts and floor accelerations for a wide range of earthquake intensities. These results suggest that the use of inerters is an attractive alternative for the seismic protection of rocking buildings. Nevertheless, further research is ongoing in order to assess the effect of the wall panel flexibility in taller structures.

Conclusions

We studied the feasibility of using supplemental rotational inertia to reduce the rotation and acceleration demands in post-tensioned rocking structures. The proposed strategy employs inerters, a mechanical device that develops a resisting force proportional to the relative acceleration between its terminals. In a first stage, a simplified single-degree-of-freedom model

was used to reveal the fundamental dynamic behaviour of post-tensioned rigid blocks equipped with inerters subjected to acceleration pulse-like excitations. Our analyses show that the vertical tendon can reduce rotational demands in rocking structures, however, it can also induce higher angular accelerations. However, the introduction of the inerter offsets this effect, decreasing the rotation response and significantly diminishing the accelerations to levels even lower than the corresponding free-standing structure. This behaviour was observed for both, single accelerations pulses and real pulse-like earthquake ground motions.

Finally, we assessed the applicability of the proposed system to real rocking building by considering the response of a 3-storey Post-tensioned CLT Walled building. To this end, numerical models of the structural system and the inerter device were developed in OpenSees, and subjected to a set of 7 pulse-like ground motions. The results of the response history analyses are consistent with the observations made for the simplified single-degree-of-freedom models. We conclude that the use of supplemental rotational inertia devices configures a practical alternative for modifying the dynamic response of rocking structures and reducing their seismic demands. However, further research is ongoing to analyse different inerter-distributions along the building height and to assess the efficiency of the system in taller structures, where the flexibility of the wall panels can be significant.

Acknowledgments

The authors acknowledge the financial support of the “Consejo Nacional de Ciencia y Tecnología” (CONICYT, Chile) for the work described in this study.

References

- Dimitrakopoulos EG, Giouvanidis AI (2018). Rocking amplification and strong-motion duration. *Earthquake Engng Struct Dyn.* 1–22.
- Giaralis A, Taflanidis A (2015). Reliability-based design of tuned mass-dampers-inerter (TMDI) equipped multi-storey frame buildings under seismic excitation. Proc., 12th Int. Conf. on Applications of Statistics and Probability in Civil Engineering, T. Haukaas, ed., Vancouver, BC, Canada.
- Housner GW (1963). The Behavior of Inverted Pendulum Structures During Earthquakes. *Bulletin of the Seismological Society of America.* 53:403-417.
- Ikago K, Saito K, Inoue M (2012). Seismic Control of Single-Degree-of-Freedom Structure Using Tuned Viscous Mass Damper. *Earthquake Engineering and Structural Dynamics,* 41:453-474.
- Makris N, Kampas G (2016). Seismic Protection of Structures with Supplemental Rotational Inertia. *Journal of Engineering Mechanics,* 142(11):1-11.
- Málaga-Chuquitaype C, Menendez-Vicente C, & Thiers-Moggia R (2019). Experimental and numerical assessment of the seismic response of steel structures with clutched inerters. *Soil Dynamics and Earthquake Engineering,* 121, 200-211.
- Mazzoni S, McKenna F, Scott M, Fenves G (2009). Open Systems for Earthquake Engineering Simulation – OpenSees version-2.1.0. Pacific Earthquake Engineering Research Center, University of California, Berkeley, CA.
- Newcombe M-P (2011). Seismic Design of Post-tensioned Timber Frame and Wall buildings. PhD thesis, University of Canterbury, New Zealand.
- Ricker N (1943). Further developments in the wavelet theory of seismogram structure. *Bull. Seism. Soc. Am.* 33(3):197–228.
- Smith M-C (2002). Synthesis of mechanical networks: The Inerter. *IEEE Trans. Autom. Control,* 47(10):1648-1662.
- Thiers-Moggia R, Málaga-Chuquitaype C (2018). Seismic protection of cross-laminated timber buildings with supplemental inertia devices. 16th European Conference on Earthquake Engineering. Thessaloniki, Greece.
- Thiers-Moggia R, Málaga-Chuquitaype C (2019). Seismic protection of rocking structures with inerters. *Earthquake Engng Struct Dyn.* 48:528–547.
- Vassiliou MF, Makris N (2015). Dynamics of the Vertically Restrained Rocking Column. *J. Eng.* 141(12):04015049.